

Escape probability of Auger electrons from noncrystalline solids: Exact solution in the transport approximation

I. S. Tilinin* and W. S. M. Werner†

Institut für Allgemeine Physik, Vienna University of Technology, Wiedner Hauptstrasse 8-10, A-1040 Vienna, Austria

(Received 31 March 1992)

The probability that an Auger electron, generated at a certain depth in a semi-infinite target, escapes from the surface under a certain emission angle is described by the so-called depth distribution function. The exact solution for this depth distribution function has been found in the transport approximation, employing transport theory. The results are in good agreement with data found in the literature and emphasize that strong deviations from exponential behavior occur. These deviations are most pronounced for oblique emission. To assess the validity of the transport approximation two kinds of Monte Carlo calculations have been performed. In one case the realistic Mott cross section for elastic scattering has been used while in the other the corresponding momentum transfer cross section was used. The latter procedure exactly fits the transport approximation. A very good agreement between the two approaches has been obtained. This indicates that the transport approximation is an effective tool in transport problems provided the angular distribution of the particle flux density varies slowly with the angle.

I. INTRODUCTION

Knowledge about the escape probability of Auger electrons from solids is of paramount importance in quantitative Auger electron spectroscopy (AES) for data interpretation and quantification. In recent years the problem has been studied extensively both theoretically and experimentally.

The experimental approach usually involves the overlayer experiment¹ and implies determination of the electron attenuation length (AL). There has been some confusion regarding the definition of this quantity and the committee *E-42* of the American Society of Testing and Materials recommends the following definition: "the average distance that an electron with a given energy travels between successive inelastic collisions as derived from a particular model in which elastic electron scattering is assumed to be insignificant." Unfortunately, the correct interpretation of data obtained by this procedure is difficult for several reasons. Firstly, an exponential attenuation law is assumed for the escape probability. Now it is evident that this assumption is not true *a priori* and serious deviations from exponential behavior can occur.^{2,3} Without quantitative knowledge concerning the attenuation law, it is difficult to extract reliable, unambiguous AL values from an overlayer experiment. Secondly, measurements of the AL by the overlayer experiment rarely have the required accuracy as there are a lot of sources of error that are not easy to evaluate properly. The standard deviation of the systematic error in independent experiments made for the same material by different authors may be around a factor 1.5 or 2.³

In the simple theoretical model widely adopted it is as-

sumed that an electron moves in matter along a straight line. According to this so-called straight line approximation the effective escape depth of particles should be fully determined by the inelastic mean free path (IMFP). Thus the effects of elastic scattering are assumed to be negligible and the values of the AL and the IMFP will be the same. However, investigations performed by a number of authors⁴⁻⁹ show that an AL measured experimentally may be less than the IMFP by up to 30% owing to elastic electron scattering.

Mathematically the escape probability is described by the depth distribution function (DDF). This function describes the probability that an electron generated at a certain depth will escape from a semi-infinite substrate without being inelastically scattered. The data obtained by the Monte Carlo technique^{10,11} indicate that the depth distribution function has a complex behavior. For any emission angle the depth distribution function exhibits a gradual change in slope as the depth increases. The slope is small in the surface near region and reaches a greater value at some larger depths for normal emission while the opposite is true in the case of oblique emission angles. Therefore it follows that elastic scattering may essentially modify the simple exponential dependence of the escape probability so that even the AL concept itself becomes questionable.

Having thoroughly analyzed their Monte Carlo data, Werner *et al.*¹¹ have proposed an empirical formula for the depth distribution function. It takes into account the randomization of electrons, which is the dominant effect at large depths, and the transition to an approximate straight line regime in the surface near region. This empirical function is in good agreement with the Monte

Carlo results for the depth distribution function. Nevertheless, some assumptions which had to be made in order to derive this formula are difficult to substantiate rigorously. In this connection the transport theory approach is worth paying attention to.

The Auger and photoelectron transport problem has been investigated analytically by means of kinetic equation solutions found in the diffusion approximation.^{6,12} Among the obtained results we note the following ones: (1) in the case of weak absorption

$$\lambda_{tr} \ll \lambda_i, \quad (1)$$

where λ_{tr} and λ_i are the transport and inelastic mean free path, respectively, the effective escape depth is proportional to⁶ $(\lambda_{tr}\lambda_i)^{1/2}$; (2) the angular distribution of escaping Auger electrons differs from a cosinoidal one and is stretched out in the forward direction, i.e., along the surface normal.¹² One should keep in mind, however, that the diffusion or P_1 approximation is only valid provided condition (1) is true, which is rarely fulfilled in the relevant Auger electron energy range. Besides, this approximation does not allow one to solve a boundary problem correctly since any limited set of Legendre polynomials does not form a fundamental system of transport equation solutions.

The boundary problem for a half-space can be solved exactly by the integral equations technique^{13,14} or the singular eigenfunction method of Case.¹⁵ For Auger electrons reasonable results can be expected in the so-called transport approximation (TA) when a realistic scattering cross section is replaced by an isotropic one equal to the transport cross section. Such replacement is justified if the radiation fields corresponding to the exact and approximate solutions are similar.¹⁴ It is obvious that the Auger electrons meet the latter requirement since their initial angular distribution is isotropic. It should also be emphasized that all the results obtained in the P_1 approximation follow from the corresponding transport approximation expressions in limit (1).^{15,16}

The scope of the present paper will be as follows: first the exact solution to the problem of the Auger electron escape probability will be derived in the transport approximation. Although it is generally accepted that this is a reasonable approximation for this specific problem, the accuracy of this approximation is difficult to assess theoretically. Therefore a detailed comparison will be presented of the transport approximation with a case in which the realistic Mott cross section for elastic scattering is used. This comparison is performed employing the Monte Carlo technique to model electron transport in matter. The obtained results are then compared with other data concerning the escape probability, as found in the literature.

II. THE DEPTH DISTRIBUTION FUNCTION IN THE TRANSPORT APPROXIMATION

The depth distribution function properly normalized may be defined as the product of the flux density of Auger electrons emerging from a solid without being inelastically scattered and the cosine of the emission angle.

Therefore, to find the depth distribution function analytically, one should solve the transport equation with a unit source of electron emitters at a certain depth z_0 and take into account the appropriate boundary conditions.

The exact solution of the transport equation with an arbitrary cross section for elastic scattering is rather complicated. However, in the case of the Auger emission problem satisfactory results can be achieved by applying the transport approximation.¹⁴ In this approximation it is assumed that the real elastic differential cross section may be replaced by an isotropic one being equal to the transport cross section. Such a replacement is justified for the azimuthally averaged radiation field provided the particle flux density is not highly anisotropic. The latter requirement is perfectly fulfilled for Auger electrons whose initial angular distribution may be regarded as isotropic.¹⁷

Let $N(z, \mu|z_0)$ denote the flux density of electrons moving at the depth z in the direction μ , where μ is the cosine of the polar angle with respect to the positive z axis directed inside the target. To indicate the source position, we retain the parameter z_0 in the flux density notation.

Hence the depth distribution function is defined by the following expression:

$$\Phi(z_0, \mu_0) = |\mu|N(z=0, \mu < 0|z_0), \quad (2)$$

where we introduced the variable $\mu_0 = \cos \psi$ representing the cosine of the emission angle with respect to the surface normal. Although definition (2) is formally different from that adopted in Ref. 11 it can be easily proved by means of the reciprocity theorem¹⁵ that both definitions are identical.

In the transport approximation the one-velocity Boltzmann equation for the flux density $N(z, \mu|z_0)$ in the case of plane symmetry has the form¹⁵

$$\mu \frac{\partial N}{\partial z} = - \left(\frac{1}{\lambda_i} + \frac{1}{\lambda_{tr}} \right) N + \frac{1}{2\lambda_{tr}} \int_{-1}^1 N(z, \mu'|z_0) d\mu' + \frac{1}{2} \delta(z - z_0). \quad (3)$$

Here λ_{tr} and λ_i are the transport and inelastic mean free paths, respectively. The nonuniform term containing the δ function on the right hand side of Eq. (3) corresponds to a unit source of Auger electrons.

The solution of Eq. (3) should satisfy the boundary condition

$$N(z=0, \mu > 0|z_0) = 0 \quad (4)$$

stipulating that the flux density of secondary electrons entering the target be equal to zero.

Introducing the new dimensionless variable

$$\tau = z(\lambda_i + \lambda_{tr})/\lambda_i\lambda_{tr} = z/\lambda_i^{TA} \quad (5)$$

and the single scattering albedo

$$\omega = \lambda_i(\lambda_i + \lambda_{tr})^{-1}, \quad (6)$$

we rewrite Eq. (3) and the boundary condition (4) in the form

$$\mu \frac{\partial N}{\partial \tau} + N = \frac{\omega}{2} \int_{-1}^1 N(\tau, \mu' | \tau_0) d\mu' + \frac{1}{2} \delta(\tau - \tau_0), \quad (7)$$

$$N(\tau = 0, \mu > 0 | \tau_0) = 0. \quad (8)$$

In expression (5) λ_{tr}^{TA} is the total mean free path in the transport approximation. Applying Case's method of solution¹⁵ to the problem, (7) and (8), we find

$$N(\tau = 0, \mu < 0 | \tau_0) = \frac{1}{2} H(-\mu, \omega) \left\{ \frac{(\nu_0^2 - 1) \exp(-\tau_0/\nu_0)}{(\nu_0 + \mu) H(\nu_0, \omega) [1 + \nu_0^2(\omega - 1)]} + \int_0^1 \frac{\phi_\nu(-\mu) g(\nu, \omega)}{\nu H(\nu, \omega)} \exp(-\tau_0/\nu) d\nu \right\}. \quad (9)$$

In the latter expression $H(\mu, \omega)$ is the H function of Chandrasekhar¹⁸ for an isotropically scattering medium, ν_0 is the positive root of the characteristic equation

$$1 = \frac{\omega \nu_0}{2} \ln \frac{\nu_0 + 1}{\nu_0 - 1}, \quad (10)$$

$\phi_\nu(\mu)$ is the eigenfunction of a continuous set ($0 \leq \nu \leq 1$)

$$\phi_\nu(\mu) = \lambda(\nu) \delta(\nu - \mu) + (\omega \nu / 2) P \frac{1}{\nu - \mu} \quad (11)$$

and

$$g(\nu, \omega) = \left\{ \left(\frac{\omega \pi \nu}{2} \right)^2 + \lambda^2(\nu) \right\}^{-1}. \quad (12)$$

In expressions (11) and (12), P refers to the Cauchy principal value and the definition

$$\lambda(\nu) = 1 - (\omega \nu / 2) \ln \frac{1 + \nu}{1 - \nu} \quad (13)$$

is used.

Putting $\mu_0 = -\mu$ and using definition (2) we obtain

$$\begin{aligned} \Phi(\tau_0, \mu_0) &= (\mu_0 / 2) H(\mu_0, \omega) \\ &\times \left\{ \frac{(\nu_0^2 - 1) \exp(-\tau_0/\nu_0)}{(\nu_0 - \mu_0) H(\nu_0, \omega) [1 + \nu_0^2(\omega - 1)]} \right. \\ &\quad \left. + \int_0^1 \frac{\phi_\nu(\mu_0) g(\nu, \omega)}{\nu H(\nu, \omega)} \exp(-\tau_0/\nu) d\nu \right\}. \end{aligned} \quad (14)$$

To analyze the depth behavior of the depth distribution function it is convenient to transform expression (14) in the following way:

$$\begin{aligned} \Phi(\tau_0, \mu_0) &= a_1(\tau_0, \mu_0) + a_2(\mu_0) \exp(-\tau_0/\mu_0) \\ &\quad + a_3(\mu_0) \exp(-\tau_0/\nu_0), \end{aligned} \quad (15)$$

where

$$a_1(\tau_0, \mu_0) = \frac{\mu_0 H(\mu_0, \omega)}{2} \int_0^1 \frac{f(\nu, \tau_0) - f(\mu_0, \tau_0)}{\nu - \mu_0} d\nu, \quad (16)$$

$$f(\nu, \tau) = \frac{\omega g(\nu, \omega)}{2H(\nu, \omega)} \exp(-\tau_0/\nu), \quad (17)$$

$$a_2(\mu_0) = \frac{1}{2} g(\mu_0, \omega) \left[1 - \frac{\omega \mu_0}{2} \ln \frac{(1 + \mu_0) \mu_0}{(1 - \mu_0)^2} \right], \quad (18)$$

$$a_3(\mu_0) = \frac{\mu_0}{\nu_0 - \mu_0} \frac{H(\mu_0, \omega)}{H(\nu_0, \omega)} \frac{\nu_0^2 - 1}{2[1 + \nu_0^2(\omega - 1)]}. \quad (19)$$

To derive Eq. (15) we used definition (11) for the eigenfunctions $\phi_\nu(\mu)$ of the continuous set.

As follows from (15) the depth distribution function consists of three terms. Each of them allows for a simple physical interpretation. The function $a_1(\tau_0, \mu_0)$ equals zero at $\tau_0 = 0$ and decreases at large depths $\tau_0 \gg 1$ proportionally to $E_1(\tau_0) \sim \exp(-\tau_0)/\tau_0$, where $E_1(\tau_0)$ is the integral exponential function. Therefore the first term describes the electrons undergoing multiple elastic scattering at arbitrary angles and escaping from the surface layer with a thickness of the order of the total mean free path λ_t^{TA} .

The second term corresponds to the Auger electrons leaving the solid without any elastic scattering (in the framework of the transport approximation). The signal intensity of these electrons is governed by the exponential factor $\exp(-\tau_0/\mu_0)$. One should keep in mind that in reality the second group of particles includes electrons participating in multiple small angle scattering processes which are neglected in the approximation considered.

The last term in (15) is represented as a product of two functions. One of them depends only on the angular variable μ_0 while the other depends on the depth τ_0 . The slope of the exponent in this case is determined by the diffusion length

$$\lambda_a = \nu_0 \lambda_i \lambda_{tr} (\lambda_i + \lambda_{tr})^{-1}. \quad (20)$$

It is obvious that the third term describes the escape probability of the fraction of randomized electrons. The diffusion length λ_a is greater than the total mean free path λ_t^{TA} since the quantity ν_0 is always larger than unity.

A thorough analysis of Monte Carlo data has shown that the parameter λ_a governs the attenuation of electrons in solids.¹⁹ Therefore it was proposed to call this quantity the attenuation parameter.

At this stage it seems advisable to point out that for the most relevant Auger electron energy range (200–2000 eV), the single scattering albedo ω is relatively small $\omega \lesssim 0.4$ and the eigenvalue ν_0 only slightly differs from unity:

$$\nu_0 \simeq 1 + 2e^{-\frac{2}{\omega}} \quad (\omega \leq 0.4).$$

The typical ν_0 values are such that $\nu_0 - 1 \sim (10^{-2} - 10^{-3})$ and the total mean free path λ_t^{TA} practically coincides with the attenuation parameter λ_a . The quantity λ_a may significantly exceed the total mean free path λ_t^{TA} only for low energies ($E < 100$ eV) in materials with a high value for the secondary electron emission coefficient (e.g., alkali halides and oxides of certain metals).

The function $\Phi(\tau_0, \mu_0)$ reaches the maximum value

$$\Phi(\tau_0 = 0, \mu_0) = \frac{1}{2}H(\mu_0, \omega)$$

at the surface and decreases monotonically while the depth τ_0 increases. The Chandrasekhar H function depends on μ_0 weakly and for small $\omega \lesssim 0.4$ is close to unity. This is clearly seen from the approximate expression for the H function²⁰

$$H(\mu, \omega) \approx \frac{1 + \mu\sqrt{3}}{1 + \mu\sqrt{3}(1 - \omega)}. \quad (21)$$

The accuracy of expression (21) is within 1.5–2.0% in the range $0 \leq \mu \leq 1$ and $\omega \lesssim 0.4$. The mentioned weak dependence of the H function on μ_0 partly justifies the semiempirical assumption made in Ref. 11 according to which $\Phi(\tau_0 = 0, \mu_0)$ is independent of μ_0 .

Further analysis concentrates on two limiting cases $\mu_0 = 1$ and $\mu_0 \ll 1$ that permit one to follow the main features of the depth distribution function.

First we consider the case $\mu_0 = 1$ assuming for simplicity that the single scattering albedo is sufficiently small. Substituting $\mu_0 = 1$ into (15) we find that the second term is zero while the first one reduces to

$$a_1(\tau_0, \mu_0) = -\frac{1}{2}H(1, \omega)(\omega/2) \times \int_0^1 \frac{d\nu}{1 - \nu} \frac{g(\nu, \omega)}{H(\nu, \omega)} \exp(-\tau_0/\nu). \quad (22)$$

For small $\omega \leq 0.1$ the function $g(\nu, \omega)$ exhibits a sharp maximum at $\nu \simeq 1/\nu_0$ so that the integration in (22) may be performed analytically. To show this we note that the main contribution to integral (22) is supplied by the integration region near the point $\nu \simeq (1/\nu_0) \simeq 1$. Introducing the new variable

$$x = -\ln(1 - \nu)$$

we may put

$$g(\nu, \omega) = \left\{ \left(\frac{\pi\omega}{2} \right)^2 + \left[1 - \frac{\omega}{2}(\ln 2 + x) \right]^2 \right\}^{-1}. \quad (23)$$

On the other hand, to avoid overestimation of the integral by a slightly increased contribution of small ν values and to fit the correct surface value of the depth distribution function we put $H(\nu, \omega) \approx H(1, \omega) \approx 1$ in the integrand. After performing these operations and integrating over x we get

$$a_1(\tau_0, 1) = \frac{1}{2}H(1, \omega) \left(1 - \frac{2}{\omega} \right) e^{-\tau_0}. \quad (24)$$

On the assumption $\nu_0 - 1 \ll 1$ we have for the coefficient $a_3(\mu_0 = 1)$

$$a_3(\mu_0) = H(1, \omega)/\omega. \quad (25)$$

Thus taking into account (16), (24), and (25), we find

$$\Phi(\tau_0, 1) = \frac{1}{2}H(1, \omega)e^{-\tau_0} \quad [\tau_0 \ll (\nu_0 - 1)^{-1}]. \quad (26)$$

From the obtained result it follows that the escape probability in the direction along the surface normal is described by a simple exponential law. Moreover, in the most important depth region the ratio $2\Phi(\tau_0, 1)/H(\nu, \omega)$ is a universal function of the reduced depth τ_0 . The above is a special case of the more general statement that in the limit of small ω the straight line regime is attained. Considering that for $\omega \rightarrow 0$ we have $\lambda_{tr} \rightarrow \infty$, $\nu_0 \rightarrow 1$, $\lambda_a \rightarrow \lambda_i$, it is immediately seen that Eq. (15) reduces to the conventionally used exponential depth distribution function which does not account for the effects of elastic scattering:

$$\Phi(z, \mu_0) = \frac{1}{2} \exp(-z/\lambda_i \mu_0). \quad (27)$$

For the medium single scattering albedo values $\omega \sim (0.3 - 0.5)$, the simple exponential law (26) is reached at larger depths. In this case the slope of the depth distribution function near the surface is gentler (usually 20% less) than that deep inside the target. It should be emphasized that this region of ω is of main interest for AES and x-ray photoemission spectroscopy (XPS).

In the opposite limiting case $\mu_0 \ll 1$, ($\nu_0 - 1 \ll 1$) one should distinguish three regions. Near the surface ($\tau_0 \leq \mu_0 \ln \frac{1}{\mu_0}$) the second term in Eq. (15) plays a leading role. The slope of the depth distribution function at these depths is very steep as the escape probability is determined by electrons leaving the target without elastic scattering (or suffering only small angle scattering). The first and second terms are small owing to the factor μ_0 .

As the depth τ_0 increases the second term diminishes rapidly. The first term becomes dominant in the depth interval $\mu_0 \ln \frac{1}{\mu_0} < \tau_0 \ll (\nu_0 - 1)^{-1}$ while the third term remains small on the assumption $\nu_0 - 1 \ll 1$. The randomized fraction of electrons begins to play a role at very large depths $\tau_0 \gg (\nu_0 - 1)^{-1} \gg 1$. It should be emphasized that this situation changes radically if the difference $\nu_0 - 1 \geq 1$. In the latter case the diffusion region is reached already for $\tau_0 \gtrsim \nu_0$ and the main contribution to the total Auger electron yield is given by diffusively scattered particles.

Hence it follows from the above considerations that for small values of the cosine of the emission angle the depth distribution function should exhibit a rapid decline near the surface and a much gentler slope at greater depths.

In conclusion we consider some integral characteristics of the escape probability. Integrating the depth distribution function over the depth we obtain the angular distribution of signal electrons

$$Y(\mu_0) = \int_0^\infty \Phi(\tau_0, \mu_0) d\tau_0 = \frac{\mu_0 H(\mu_0, \omega)}{2\sqrt{1 - \omega}}. \quad (28)$$

Due to the weak dependence of the H function on μ_0 the angular distribution (28) is practically cosinusoidal for $\omega \lesssim 0.5$. In the case of intensive scattering $\lambda_{tr} \ll \lambda_i$ and $\omega \approx 1$ the angular distribution (28) is somewhat stretched forward along the surface normal. However, for Auger electrons the assumption made in Ref. 11 that

the angular distribution is cosine shaped is valid to a good approximation.

Let A denote the amount of Auger electrons generated in a unit volume of matter per unit time. Multiplying (28) by $A\lambda_e^{\text{TA}}$ and integrating the resulting expression over the emission angle, we find for the total Auger emission yield

$$Y = A\lambda_{\text{tr}} \left[\nu_0 - 1 + \frac{1}{\pi} \int_0^1 \arctan \left(\frac{\pi\omega\mu}{2\lambda(\mu)} \right) d\mu \right]. \quad (29)$$

The quantity Y represents the amount of electrons escaping from a unit area of the target surface in a unit time.

For the most interesting case $\omega \lesssim 0.4$ we may neglect the difference $\nu_0 - 1$ in the large square brackets in Eq. (29) and replace the function $\arctan(x)$ by its value at small arguments

$$\arctan \frac{\pi\mu\omega}{2\lambda(\mu)} \approx \frac{\pi\mu\omega}{2}. \quad (30)$$

Substitution of (30) into (29) gives the following expression for the total yield:

$$Y \approx \frac{1}{4} A\lambda_{\text{tr}}\lambda_i(\lambda_{\text{tr}} + \lambda_i)^{-1}. \quad (31)$$

The accuracy of this expression is about 20% in the worst case of $\omega = 0.4$.

From (31) it follows that in the limiting case $\lambda_{\text{tr}} \gg \lambda_i$ the total yield Y is proportional to the inelastic mean free path, in accordance with the straight line approximation, which neglects elastic scattering. Therefore we emphasize that the transport approximation provides a correct quantitative description of the escape probability even if $\lambda_{\text{tr}} \gg \lambda_i$.

The opposite limiting case $\lambda_{\text{tr}} \ll \lambda_i$ seems to be less important because of the corresponding electron energy range extending from few to hundred electronvolts. Nevertheless we note that for $\lambda_{\text{tr}} \ll \lambda_i$ the total yield depends on the mean geometrical of λ_{tr} and λ_i ,

$$Y \sim A(\lambda_{\text{tr}}\lambda_i)^{1/2}, \quad (32)$$

since the eigenvalue of a discrete set increases proportionally to $(\lambda_{\text{tr}}\lambda_i)^{1/2}$.

III. COMPARISON WITH OTHER CALCULATIONS

The applicability of the results in the previous section depends on the accuracy of the considered approximation, i.e., the transport approximation. Since it is difficult to analyze the accuracy of this approximation analytically, we have performed a numerical comparison between the exact case and the approximate one, employing the Monte Carlo technique.

In the transport approximation, the exact cross section is replaced by a pseudoisotropic transport cross section:

$$N_0\sigma_{\text{tr}}(\mu) = \left(\frac{1}{\lambda_e} - \frac{1}{\lambda_{\text{tr}}} \right) \delta(1 - \mu) + \frac{1}{2\lambda_{\text{tr}}}, \quad (33)$$

where N_0 is the atomic density of the material, λ_e denotes

the elastic mean free path and λ_{tr} is given by

$$1/N_0\lambda_{\text{tr}} = \sigma_{\text{tr}} = 2\pi \int_{-1}^1 \frac{d\sigma_e(\mu)}{d\mu} (1 - \mu) d\mu. \quad (34)$$

The factor $(1 - \mu)$ in Eq. (34) emphasizes backscattering and the choice of the parameters in Eq. (33) preserves the correct total elastic scattering strength.

It is obviously very simple to incorporate a scattering process of the form Eq. (33) into a Monte Carlo algorithm for electron transport. It suffices to replace the elastic mean free path by the transport mean free path (stipulating that forward scattering be the dominant feature in the cross section for elastic scattering) and, furthermore, to assume that the cosine of the scattering angles is uniformly distributed in the range $[-1, 1]$. The details of the employed algorithm can be found elsewhere,¹¹ we merely note here that the relativistic differential Mott cross sections calculated with the partial wave expansion method²¹ were used for the calculation of the exact depth distribution function.

The most interesting Auger electron energy range corresponds to the region $0.1 \leq \omega \leq 0.5$, while typically $\omega \sim 0.3$. In Fig. 1 an example for a low ω case, viz., 1000-eV electrons in Be is shown as a semilogarithmic plot of the depth distribution function versus the reduced depth, for different emission angles (0° , 60° , and 80°). All curves shown have been normalized to unity at $\tau_0 = 0$. The values for the IMFP were calculated from the formula of Tanuma, Powell, and Penn.²² Since this case is close to the straight line approximation limit $\omega \rightarrow 0$, the agreement between the transport approximation and the exact approach is very good, as expected. For small emission angles ($\mu = 1, 0.5$) the agreement is almost perfect, while for $\mu = 0.174$ the transport approximation results are slightly higher than the exact values for $\tau_0 < 1$ while the opposite is observed for larger depths. The depth distribution function for normal emission supports the universal exponential relation for the depth distribution

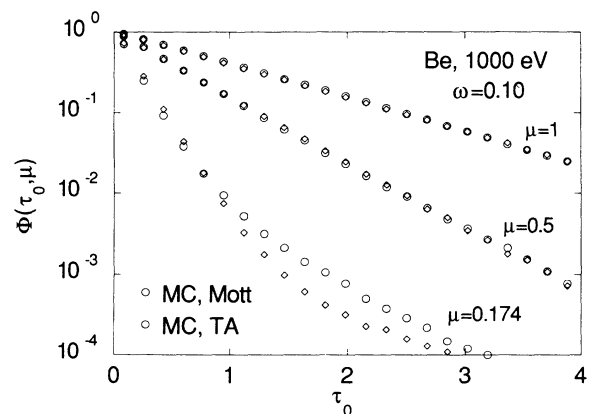


FIG. 1. The depth distribution function for 1000-eV electrons in Be ($\omega = 0.10$), calculated by means of a Monte Carlo algorithm for the transport of electrons in matter, using (○), the relativistic Mott cross section for elastic scattering (Ref. 21) and (◇), the corresponding transport cross section.

function in the transport approximation Eq. (26), valid for small ω .

A case with a relatively high value of $\omega = 0.42$ is shown in Fig. 2, i.e., the depth distribution function for 250-eV electrons in Co. Here the differences between the transport approximation and the exact calculation are more pronounced, although still far from severe. For 80° the same effect is seen as in Fig. 1, viz., the transport approximation depth distribution function is slightly higher than the exact one for $\tau_0 < 1$ and vice versa for larger depths. For the other emission angles the transport approximation depth distribution function is slightly lower than the exact one over the entire depth range considered. The universal relation Eq. (26) does not hold for this rather large value of ω , since as can be seen, the depth distribution function at normal emission deviates from an exponential form.

An example for a typical value of $\omega = 0.32$ is shown in Fig. 3, for 1000-eV electrons in Ag. The same effects as in the previous example can be seen, although less pronounced. As regards the validity of the transport approximation we conclude that it is a very accurate and effective approximation in the case of Auger electrons ($0.1 \lesssim \omega \lesssim 0.5$).

The exact solution of the depth distribution function in the transport approximation Eq. (15), calculated numerically, is also shown in this figure as dashed lines. The agreement between this exact solution and the Monte Carlo data using the transport cross section is excellent. The solid lines in this figure represent the empirical depth distribution function of Werner *et al.*,¹¹ derived from a detailed analysis of their Monte Carlo results. A closer comparison of this empirical depth distribution function with the present results seems interesting at this point.

These authors performed a detailed statistical analysis of the depth distribution function calculated by the Monte Carlo technique and by imposing certain normalization conditions they found a semiempirical analytical expression for the depth distribution function which reads (in the present notation)¹¹

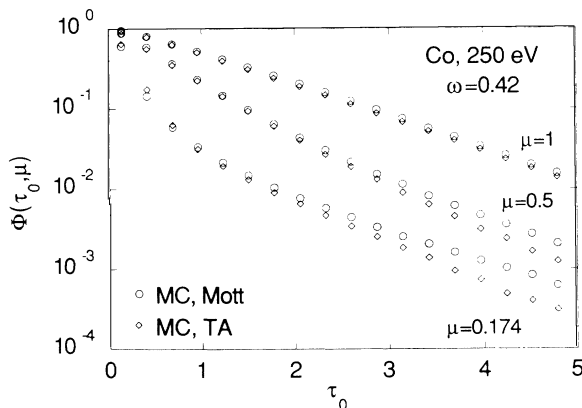


FIG. 2. Same as Fig. 1 for 250-eV electrons in Co ($\omega = 0.42$).

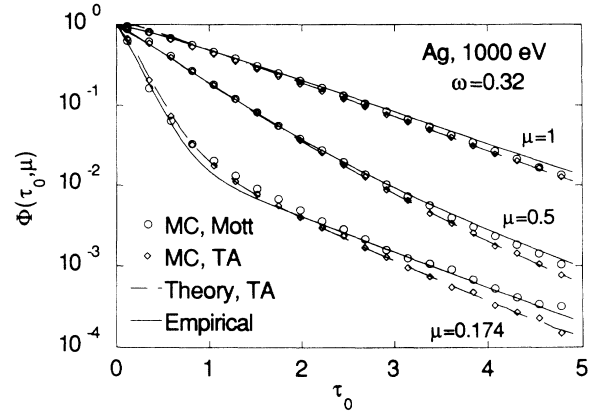


FIG. 3. Same as Fig. 1 for 1000-eV electrons in Ag ($\omega = 0.32$). The dashed lines represent the theoretical depth distribution function in the transport approximation Eq. (15), the solid lines are the empirical depth distribution function Eq. (35) (Ref. 11).

$$\begin{aligned} \Phi(\tau_0, \mu_0) = & -a_1 \exp(-\tau_0 \lambda_t^{\text{TA}} / \mu_0 \lambda_t) \\ & + a_2(\mu_0) \exp(-\tau_0 / \mu_0 \nu_0) \\ & + a_3(\mu_0) \exp(-\tau_0 / \nu_0), \end{aligned} \quad (35)$$

where

$$a_1 = \left(\frac{\lambda_t}{\lambda_i} \right) \left(\frac{\lambda_i - \lambda_a}{\lambda_a - \lambda_t} \right), \quad (36)$$

$$a_2(\mu_0) = 1 + a_1 - a_3(\mu_0), \quad (37)$$

$$a_3(\mu_0) = \frac{\mu_0}{1 - \mu_0} \left(\frac{\lambda_t}{\lambda_i} \right) \left(\frac{\lambda_i - \lambda_a}{\lambda_a} \right). \quad (38)$$

Moreover, these authors found that the total yield Y is given by

$$\frac{Y}{A} = \lambda_a + 2 \left(\frac{\lambda_t}{\lambda_i} \right) (\lambda_i - \lambda_a). \quad (39)$$

In Eqs. (36)–(39) λ_t denotes the total mean free path $\lambda_t = 1/N_0(\sigma_e + \sigma_i)$ where σ_i is the inelastic cross section. Remembering that for the relevant electron energy range we have $0 \leq \omega \leq 0.5$, implying that $1.00 \leq \nu_0 \leq 1.04$, it is easily seen that the angular dependence of Eq. (38) and Eq. (19) and the depth dependence of the latter two terms of Eq. (35) and Eq. (15) practically coincide. It is clear that the subtle difference between the total mean free path and the diffusion length (by a factor $\nu_0 \approx 1.00$), which also causes the slight difference in the angular dependence of a_3 , could not have been extracted from an analysis of Monte Carlo data. The first term in Eq. (35) is difficult to substantiate with the aid of the present results. The depth region where the first term contributes depends on the quantity $\lambda_t^{\text{TA}}/\lambda_t$ which is in the range (1.1–3.0) for Auger electrons. The empirical depth distribution function Eq. (35) is also shown in Fig. 3 for comparison. The features in the exact depth distribution function are reproduced with good accuracy by Eq. (35), and the differences between the exact and the trans-

TABLE I. The ratio of the electron yield for an emission angle $\mu_0 = 0.78$ with and without elastic scattering for a few pronounced Auger transitions (see text).

Transition	Energy (eV)	ω	$q_{\text{Jablonski}}$ (Ref. 23)	Eq. (39)	Eq. (28)
C <i>KLL</i>	272.00	0.28	0.96	0.97	0.97
Al <i>KLL</i>	1396.00	0.23	0.99	1.00	0.98
Si <i>KLL</i>	1618.00	0.20	0.99	1.00	0.98
Cr <i>LMM</i>	529.00	0.33	0.91	0.89	0.92
Fe <i>LMM</i>	703.00	0.32	0.93	0.89	0.92
Ni <i>LMM</i>	848.00	0.31	0.92	0.88	0.92
Cu <i>LMM</i>	920.00	0.29	0.92	0.89	0.93
Ge <i>LMM</i>	1147.00	0.22	0.94	0.94	0.95
Zr <i>LMM</i>	1845.00	0.20	0.97	0.95	0.96
Nb <i>LMM</i>	1944.00	0.22	0.94	0.93	0.97
Mo <i>LMM</i>	2044.00	0.23	0.95	0.92	0.96
Zr <i>MNN</i>	147.00	0.33	0.90	0.93	0.89
Nb <i>MNN</i>	167.00	0.38	0.89	0.89	0.92
Mo <i>MNN</i>	186.00	0.41	0.89	0.86	0.86
Pd <i>MNN</i>	330.00	0.30	0.87	0.87	0.89
Ag <i>MNN</i>	356.00	0.29	0.89	0.88	0.89
La <i>MNN</i>	625.00	0.28	0.91	0.92	0.93
Ta <i>MNN</i>	1680.00	0.33	0.92	0.85	0.92
W <i>MNN</i>	1736.00	0.34	0.90	0.83	0.92
Pt <i>MNN</i>	1967.00	0.34	0.90	0.83	0.90
Au <i>MNN</i>	2024.00	0.33	0.91	0.85	0.91

port approximation Monte Carlo results correspond accurately to the differences between the empirical depth distribution function Eq. (35) and the theoretical depth distribution function Eq. (15). This result suggests that the first term in Eq. (35) reflects the differences between the exact and the transport approximation cases.

As a final result we present a comparison of an integral characteristic, viz., the total electron yield, as predicted by the depth distribution function Eq. (15) with the empirical depth distribution function Eq. (35) and Monte Carlo results from Jablonski.²³

In Table I the ratio of the yield in the direction $\mu_0 = 0.78$ in the presence of elastic scattering and without it is shown for a few pronounced Auger transitions. The theoretical values were calculated with Eq. (28) using the values of the H function tabulated in Ref. 18. The values for the IMFP were the same as the ones used by Jablonski, i.e., the values of Seah and Dench.²⁴ The transport mean free path was calculated by the quasichlorical formula of Tilinin,²⁵ while the necessary total mean free paths were interpolated from the values tabulated by Werner.⁹

The agreement between Jablonski's Monte Carlo results and the semiempirical formula Eq. (35) for the electron yield is reasonable for all cases studied except for the high energy *MNN* transitions of Ta, W, Pt, and Au. The transport theory results, Eq. (28), are in excellent agreement with Jablonski's results for all cases studied. The slight discrepancies with Jablonski's results and the other results do not seem to be correlated with the value of ω .

IV. DISCUSSION

The results presented in this study reveal an interesting possibility of the application of the transport ap-

proximation to the intermediate scattering parameters $\lambda_e < \lambda_i < \lambda_{tr}$ and may prove to be useful also in astrophysical and neutron transport problems.

It is usually appreciated that the transport approximation provides good results in the case of very strong absorption $\lambda_i \ll \lambda_e, \lambda_{tr}$ and for the quasiconservative medium $\lambda_i \gg \lambda_e, \lambda_{tr}$. The former case corresponds to the trivial situation where elastic scattering is negligible and the rectilinear motion model may be used. The justification for the transport approximation for nearly conservative scattering is based on the so-called radiative field similarity principle.¹⁴ It implies that the approximate solution correctly describes the radiative field at large distances from a source and is expressed mathematically by the similarity relationships. In the transport approximation case these relationships are reduced to the simple equation

$$\lambda_a = \nu^* \lambda_t, \quad (40)$$

where ν^* is the biggest root of the general characteristic equation:

$$1 - \omega^* = \frac{(1/\nu^*)^2}{3 - \omega^* x_1 - \frac{(2/\nu^*)^2}{5 - \omega^* x_2 - \frac{(3/\nu^*)^2}{7 - \omega^* x_3 - \dots}}} \quad (41)$$

and $\lambda_t = \lambda_i \lambda_e (\lambda_i + \lambda_e)^{-1}$ is the total mean free path. In formula (41) ω^* is the usual single scattering albedo $\omega^* = \lambda_i (\lambda_i + \lambda_e)^{-1}$ while x_i is the i th coefficient in the Legendre polynomial expansion of the normalized differential elastic scattering cross section. The quantity $\nu^* \lambda_t$

is equal to the characteristic length governing the exact distribution function slope far away from the source.

The calculations show that relationship (40) holds only approximately in the relevant Auger electron energy range. However the electron transfer is fairly well described in the framework of the transport approximation. The main reason is that the similarity of the exact and the approximate solutions can be achieved not only in the case of weak absorption but also in problems with slowly varying particle angular distribution. To elucidate this we note that the main disadvantage of the transport approximation is that the specific features of electron scattering concerning the path lengths $s \ll \lambda_{tr}$ are not taken into account properly. The particles that have traveled such small path lengths are deflected mainly through small angles. They continue to move along directions close to the initial one since large angle scattering events are less probable due to the strong forward peak in the elastic cross section. Therefore it is obvious that the broad initial emission angular distribution is not considerably affected by these small angle scattering processes and also that these small angle scattering processes will not significantly influence the electron transport in the target. Therefore the shortcoming of the transport approximation mentioned above becomes unessential if the condition

$$\left| \frac{\partial \bar{N}}{\partial \mu} \right| \lesssim \bar{N} \quad (42)$$

is fulfilled. In inequality (42) \bar{N} is the typical value of the particle flux density. The Auger electrons meet the latter requirement perfectly as their initial angular distribution is isotropic. The Monte Carlo simulation data

clearly indicate that this qualitative argument also yields quantitatively correct results. The other way of checking the transport approximation is a direct comparison with the exact solution of the Auger electron transport problem. Such a comparison is beyond the scope of the present paper. Nonetheless the present preliminary results show that the error made by using the transport approximation is relatively small for both the depth and the angular dependence of the emission characteristics (cf. Fig. 3 and Table I).

V. CONCLUSIONS

We have presented a study of the Auger electron escape probability from noncrystalline solids comprising both an analytical and a Monte Carlo approach. Simple analytical expressions have been derived for several characteristics of Auger electron emission on the basis of the transport approximation. The theoretical results are in good agreement with corresponding Monte Carlo calculations. It should be emphasized that the latter have been performed for realistic Mott cross sections as well as for isotropic (transport) cross sections. Thus it has been proved that the transport approximation is an effective tool in transport problems when the particle angular distribution at the source is a slowly varying function of the angle. The important point is that no limitations are imposed on the scattering parameters in this case.

ACKNOWLEDGMENT

The authors gratefully acknowledge financial support by the Austrian Science Foundation through Project No. PHY-8558.

*On leave from Moscow Engineering Physics Institute, Uashirskoye shosse, 31, 115409 Moscow, Russia.

†Author to whom correspondence should be addressed.

¹C.J. Powell, Surf. Sci. **44**, 29 (1974).

²C.J. Powell, J. Electron. Spectrosc. Relat. Phenom. **47**, 197 (1988).

³C.J. Powell and M.P. Seah, J. Vac. Sci. Technol. **8**, 735 (1990).

⁴O.A. Baschenko and V.I. Nefedov, J. Electron. Spectrosc. Relat. Phenom. **21**, 153 (1980).

⁵O.A. Baschenko and V.I. Nefedov, J. Electron. Spectrosc. Relat. Phenom. **27**, 109 (1982).

⁶S. Tougaard and P. Sigmund, Phys. Rev. B **25**, 4452 (1982).

⁷J. Ferron, E.C. Goldberg, L.S. de Bernadez, and R.H. Buitrago, Surf. Sci. **123**, 239 (1982).

⁸V.M. Dwyer and J.A.D. Matthew, Vacuum **33**, 767 (1983).

⁹W.S.M. Werner, Surf. Interface Anal. **18**, 217 (1992).

¹⁰W.S.M. Werner, W. H. Gries, and H. Störi, J. Vac. Sci. Technol. A **9**, 21 (1991).

¹¹W.S.M. Werner, W.H. Gries, and H. Störi, Surf. Interface Anal. **17**, 693 (1991).

¹²A.L. Tofterup, Surf. Sci. **167**, 70 (1986).

¹³B. Davison, *Neutron Transport Theory* (Oxford University

Press, Oxford, 1955).

¹⁴V.V. Sobolev, *Rasseyanie Sveta v Atmosferah Planet* (Nauka, Moscow, 1972) (in Russian).

¹⁵K.M. Case and P.F. Zweifel, *Linear Transport Theory* (Addison-Wesley, Reading, MA, 1967).

¹⁶I.S. Tilinin, Poverkhnost **1**, 37 (1988) (in Russian).

¹⁷E.H.S. Burhop and W.H. Asaad, Adv. Atom Mol. Phys. **8**, 164 (1972).

¹⁸S. Chandrasekhar, *Radiative Transfer* (Dover, New York, 1960).

¹⁹W.S.M. Werner and I.S. Tilinin, Surf. Sci. **268**, L319 (1992).

²⁰A.P. Lightman and G.B. Rubicki, Astrophys. J. **236**, 928 (1980).

²¹A.C. Yates, Comput. Phys. Commun. **2**, 175 (1971).

²²S. Tanuma, C.J. Powell, and D.R. Penn, Surf. Interface Anal. **11**, 577 (1988).

²³A. Jablonski, Surf. Sci. **188**, 164 (1987).

²⁴M.P. Seah and W.A. Dench, Surf. Interface Anal. **1**, 2 (1979).

²⁵I.S. Tilinin, Zh. Eksp. Teor. Fiz. **94**, 96 (1988) [Sov. Phys. JETP **67**, 1570 (1988)].